Technical and Engineering Insights into Green Iron Production from Bauxite Residue: A Microwave Plant Assembly Process

Marcelo Montini[1], Darllan do Rosario Pinheiro[2], Raphael Vieira da Costa[3], Luis Rodolfo Mariani Bittencourt[4], Lucas Arantes Araújo[5], Amaury Jose Leone Negrao[6], Guilherme Henrique Camello do Nascimento[7] and Izabel Nunes Ivancko[8]

1. Senior Chemical Consultant
2. R&D Specialist
3. Head of Technology

Norsk Hydro Alunorte, Barcarena, Brazil

4. CTO
5. Head of R&D
6. Head of Engineering
7. R&D Coordinator
8. Engineering Specialist

New Wave, Rio de Janeiro, Brazil

Corresponding author: marcelo.montini@hydro.com

https://doi.org/10.71659/icsoba2024-br007

Abstract

Recent advancements in the production of low-carbon iron from bauxite residue have indeed yielded promising results, paving the way for sustainable iron production processes. Bench-scale and pilot-scale studies have underscored the technical and economic viability of this approach to start the microwave plant engineering for a 50 000 tpy bauxite residue capacity. Specifically, the utilization of carbon-capturing sources during growth, such as charcoal and biomass, coupled with microwave energy, has been instrumental in the reduction of iron. Moreover, the use of renewable energy sources to power microwave energy further enhances the sustainability profile of the process. The resulting iron briquette exhibits exceptional metallization, surpassing 90 %, with iron content ranging from 92 % to 95 %, and notably low sulfur and phosphorus levels. These characteristics not only meet but exceed the stringent specifications required for steel production. The reuse of bauxite residue not only minimizes waste but also creates a sustainable and economically feasible product, thus closing the lifecycle loop of alumina production. This innovative approach not only addresses environmental concerns associated with traditional iron production methods and bauxite residue handling but also offers a feasible pathway towards achieving carbon-neutral steel production. Furthermore, the material that remains after the conversion and production of pig iron, having undergone thermal conversion, exhibits interesting characteristics and is under development for use mainly in civil construction, ceramic and steelmaking sector, and other applications with high demand, potentially enabling the utilization of 100 % of the bauxite residue.

Keywords: Bauxite residue, Green iron, Microwave, Circular economy.

1. Introduction

Bauxite residue (BR) is produced as waste in alumina refineries through the Bayer process. This process was developed by Austrian chemist Karl Josef Bayer on August 3, 1888, and remains the primary method for producing alumina from diasporic, boehmitic, and gibbsite bauxite to this day, accounting for up to 90 % to the total production [1]. The bauxite residue processed by this process produce from 0.55 to 2.21 tonnes of bauxite residue per tonne of alumina produced [2] making this residue a concern to disposal due the quantity of waste generated and the hazardous characteristics of this material, the Figure 1 shows the Bayer process and the bauxite residue formation.

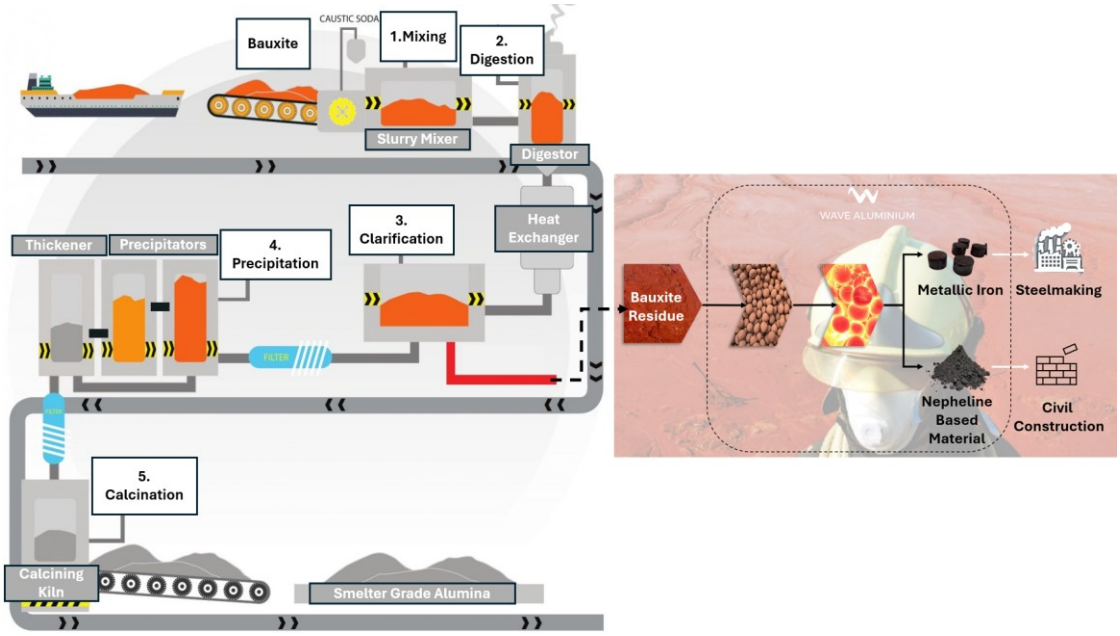

Figure 1. Main unit operations for alumina beneficiation [3] and Wave Aluminium bauxite residue beneficiation.

In the alumina production process, the main unit operations can be seen in Figure 1. The bauxite is received at the plant, crushed, and ground to an appropriate particle size to optimize aluminium extraction. After this step, it is mixed with sodium hydroxide and digested in digesters, producing sodium aluminate and bauxite residue. These are separated in settlers, where the bauxite residue is thickened, filtered using a filter press to reduce moisture, and sent to the solid waste disposal area. The sodium aluminate-rich liquor is then sent to clarifiers and precipitators, where aluminium hydroxide seed is added to precipitate aluminium hydroxide. This precipitate is then filtered and calcined in rotary kilns to produce calcined alumina, which can be used in the chemical industry for refractory production or as smelting grade alumina (SGA) to produce metallic aluminium [4]. Due to the characteristics of this process, the ore used, and the volume generated, bauxite residue has properties that make it difficult to manage. These include the need for large disposal areas, fine particle size (with most of the mass being below 20 micrometers), high pH (around 12 due to the use of sodium hydroxide in the process), and the presence in trace concentration of certain heavy metals and naturally occurring radioactive elements such as lead, mercury, uranium, and thorium [5]. The process developed by Wave Aluminium aims to remove iron from this residue and generate a co-product suitable for use in civil construction by utilizing microwave energy in beneficiation.

According to the database of the International Aluminium Institute (IAI), if no action is taken to consume bauxite residue, the accumulated amount by 2050 will be approximately 9 billion tonnes, Figure 2 [6].

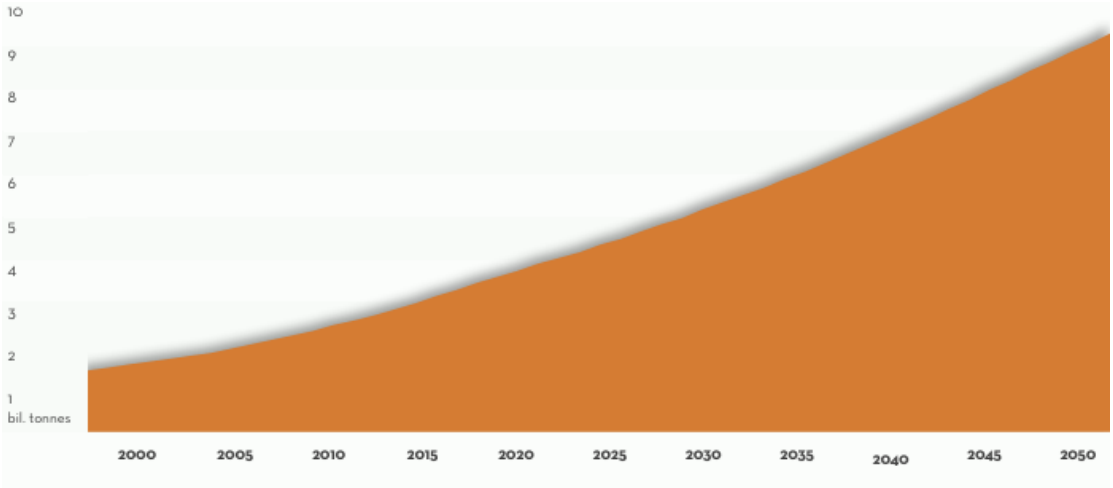

Figure 2. Estimated accumulation of bauxite residue by 2050 under current recycling scenario [6].

On June 30, 2023, the European Council added bauxite, alumina, and aluminium to the list of strategically important and critical materials list, with aluminium demand set to increase by 30 % by 2040 [7]. This will put pressure on production, generating more bauxite residue and continuing the upward trend in residue generation, making it even more urgent to find a solution for this waste.

Due to the large volume of material generated and the composition discussed in the previous sections, interest in recycling bauxite residue has been growing rapidly in both academic and industrial environments. The number of publications from the leading countries researching in this area – Italy, Hungary, Canada, South Korea, the United Kingdom, Brazil, Turkey, the United States, Australia, India, and China – has been increasing each decade. There were about 25 publications in the early 2000s, 150 in the early 2010s, 450 in 2021, and nearly 600 in 2023. This accelerated pace reflects the academic and industrial pursuit, as part of these publications result from industry partnerships, to address this environmental liability [2].

On the other hand, the effective use of large volumes of bauxite residue remains stagnant. According to the International Aluminium Institute's report titled "Bauxite Residue: An Introduction" from September 2022, it is estimated that the global amount recycled per year is approximately 2.5 to 5 million tonnes, representing less than 3 % recycling. Almost all of this percentage is used as a substitute for clinker in Portland cement [8].

Based on this scenario, a definitive solution for utilizing bauxite residue must address environmental, economic, and supply aspects. It should generate value-added products, reduce the carbon footprint, and the product must be used in large quantities by other industries.

1.1 Bauxite Residue Composition

The composition of bauxite residue can vary depending on the type of bauxite ore used, the amount of macroconstituents in the bauxite, and the refining conditions. The oxide and mineral composition can vary significantly within the range shown in Table 1 [2]; bauxite residue is predominantly composed of iron oxides, mainly in the form of Al-goethite, where some aluminium substitution in the goethite crystal structure can be observed, as well as hematite and magnetite.

Table 1. Average Composition of Oxides and Minerals in Bauxite Residue [2].

Oxide	Typical range (wt %)	Minerals	Typical range (wt %)
Fe_2O_3	5 - 60	Sodalite ($3Na_2O.3Al_2O_3.6SiO_2.Na_2SO_4$)	4 - 40
Al_2O_3	5 - 30	Al-goethite ($(Fe,Al)_2O_3.nH_2O$)	1 - 55
TiO_2	0.3 - 15	Hematite (Fe_2O_3)	10 - 30
CaO	2 - 14	Magnetite (Fe_3O_4)	0 - 8
SiO_2	3 - 50	Silica (SiO_2) crystalline and amorphous	3 - 20
Na_2O	1 - 10	Calcium aluminate ($3CaO.Al_2O_3.6H_2O$)	2 – 20
		Boehmite (AlOOH)	0 – 20
		Titanium Dioxide (TiO_2) anatase and rutile	2 – 15
		Muscovite ($K_2O.3Al_2O_3.6SiO_2.2H_2O$)	0 – 15
		Calcite ($CaCO_3$)	2 – 20
		Kaolinite ($Al_2O_3.2SiO_2.2H_2O$)	0 – 5
		Gibbsite ($Al(OH)_3$)	0 – 5
		Perovskite ($CaTiO_3$)	0 – 12
		Cancrinite ($Na_6[Al_6Si_6O_{24}].2CaCO_3$)	0 – 50
		Diaspore (AlOOH)	0 – 5

This makes the residue a potential raw material for the steel industry as a source of iron. Aluminium follows, present in the form of sodalite, resulting from the reprecipitation of kaolinite structure during the Bayer digestion forming this desilication product (DSP) [10], and as boehmite, gibbsite, and diaspore, which relate to the inefficiency of the process. Another important component is silica, which can be in the crystalline form of quartz, amorphous form (from reactive silica), and as sodalite. Another significant constituent is sodium, almost entirely derived from the sodium hydroxide added in the Bayer process. These, along with calcium and titanium, compose almost the entirety of the residue [2]. In addition to these macroconstituents, rare earth elements (including scandium), gallium, uranium, and thorium are also present as microconstituents, which, depending on their concentration, may have commercial interest.

1.2 Microwave Assisted Metallurgy

One of the ways to achieve large-scale use of bauxite residue is to remove its major components. Iron, for example, accounts for 40 to 60 % of the total residue in most cases [2]. Therefore, removing iron results in a substantial reduction in mass, as the reduction process eliminates moisture, water from the crystal structure, and oxygen during the reduction steps.

There are some difficulties in reducing bauxite residue under existing ironmaking conditions. The presence of free sodium can alter the alkali balance, increasing the coke ratio in a blast furnace and consequently increasing the consumption of reducing agents. Studies concluded that each kilogram increase in alkali input in blast furnace increases fuel consumption by 3.2 kg per tonne of iron produced [11]. This occurs because the process operates at temperatures above the melting point of iron to ensure slag separation by density difference. Another drawback of using the residue in conventional ironmaking is that the sodium content attacks the refractory lining, increasing wear. To achieve effective iron reduction with technical and economic feasibility, the development of new reduction technologies is necessary.

Jovičević-Klug et al. [12] presented a concept for utilizing the iron present in bauxite residue using hydrogen plasma. This work is at the lab scale, with approximately 15 grams per experiment, and has shown to be technically feasible for iron reduction.

According to Angel Lopez in the report "Demonstration of BR microwave roasting in prototype furnace (2023)", a plant for processing 30 kg/h using microwaves for iron conversion generates magnetite, nuggets, and small pellets depending on the conversion conditions [13]. This plant uses a rotary kiln, and a challenge with these types of furnaces is the propagation and dispersion of microwaves because these pieces of equipment are long.

Microwave technology for the reduction of iron oxides could be a viable alternative to promote reduction and subsequent separation. The main reactions involved in the reduction of iron can be seen below [14-17].

$$FeOOH \leftrightarrow Fe_2O_3 + H_2O \qquad \Delta H = -561.5\ kJ/mol \qquad (1)$$
$$3Fe_2O_3 + CO \leftrightarrow 2Fe_3O_4 + CO_2 \qquad \Delta H = -41.8\ kJ/mol \qquad (2)$$
$$Fe_3O_4 + 4CO \leftrightarrow 3Fe_{(product)} + 4CO_2 \qquad \Delta H = -13.6\ kJ/mol \qquad (3)$$
$$Fe_3O_4 + 4CO \leftrightarrow 3FeO + 4CO_2 \qquad \Delta H = +19.4\ kJ/mol \qquad (4)$$
$$FeO + CO \leftrightarrow Fe_{(product)} + CO_2 \qquad \Delta H = -11.0\ kJ/mol \qquad (5)$$
$$C + O_2 \leftrightarrow CO_2 \qquad \Delta H = -394.96\ kJ/mol \qquad (6)$$
$$CO_2 + C \leftrightarrow 2CO \qquad \Delta H = 172\ kJ/mol \qquad (7)$$

Where:
ΔH = Enthalpy under standard conditions (298 K).
$FeOOH$ = goethite.
Fe_2O_3 = hematite.
Fe_3O_4 = magnetite.
FeO = wustite.
Fe = metallic iron (product).
C = carbon.
CO = carbon monoxide.
CO_2 = carbon dioxide.
O_2 = oxygen.

The reduction reaction of iron oxides, Figure 3, begins with the combustion of the carbon source, producing carbon dioxide (Reaction 6). This step heats the reaction medium as the reaction is largely exothermic, releasing heat as it occurs. This heating induces the dihydroxylation of goethite, which starts to occur around 250°C, and contributes to the temperature increase. The CO_2 formed reacts with carbon again, forming CO gas, which is the reducing gas that promotes the reduction of iron oxides to metallic iron. Below approximately 570 °C and under Boudouard equilibrium conditions (approximately 50 % CO and 50 % CO_2), the reduction reaction will proceed via Equations (2) and (3). Above this temperature or with a low CO/CO_2 ratio, the reduction occurs via Equations (2), (4) and (5), passing through the intermediate wustite phase, indirect reduction [15].

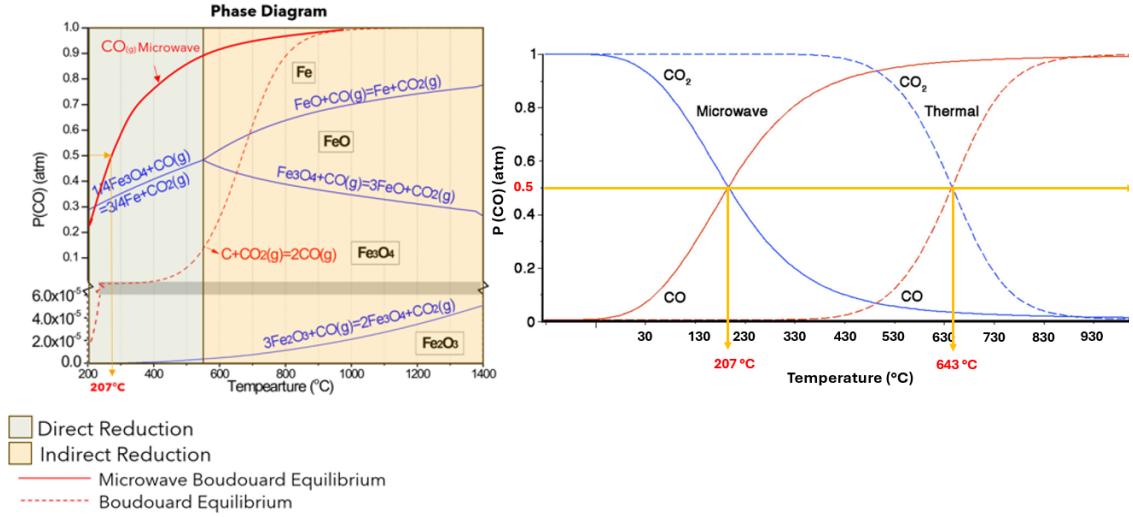

Figure 3. Left: The phase diagram shows the stable phases of iron according to the partial pressure ratio of P(CO) or ($CO/CO+CO_2$) by temperature, with the Boudouard reaction without microwave irradiation plotted with a red dashed line and with microwave irradiation plotted with a solid line (modified from reference [17]), Right: Boudouard equilibrium under microwave irradiation (solid lines) and without (thermal, dashed lines) (modified from reference [18]).

As discussed, and concluded by Jacob Hunt et al. in the article "Microwave-Specific Enhancement of the Carbon-Carbon Dioxide (Boudouard) Reaction," the Boudouard reaction (7), which governs the reduction of iron oxides, is specifically enhanced by microwave irradiation. Under conditions without microwave use, the reaction is largely endothermic, with the equilibrium shifted towards CO_2 formation. This equilibrium shifts to high temperatures, above 643 °C, where the Gibbs free energy of the reaction becomes negative, favouring CO formation. Under microwave irradiation, this reaction has an equilibrium well below the conventional thermal process, with the apparent activation energy dropping more than 5 times, achieving equilibrium in CO formation at 207 °C, which is desirable in the reduction process via intermediates (2) and (3), direct reduction [18].

This, combined with the fact that different materials have different interactions with microwave energy, enables the reduction and agglomeration of iron in bauxite residue, even with lower iron oxide content.

2. Methodology

Hydro Alunorte and Wave Aluminium (subsidiary of New Wave) has an agreement to set up the first demonstration plant for bauxite residue beneficiation using microwave technology, with engineering designed for a capacity of 50 000 tonnes per year. The methodology used for the development of the technology and process engineering can be observed in Figure 4.

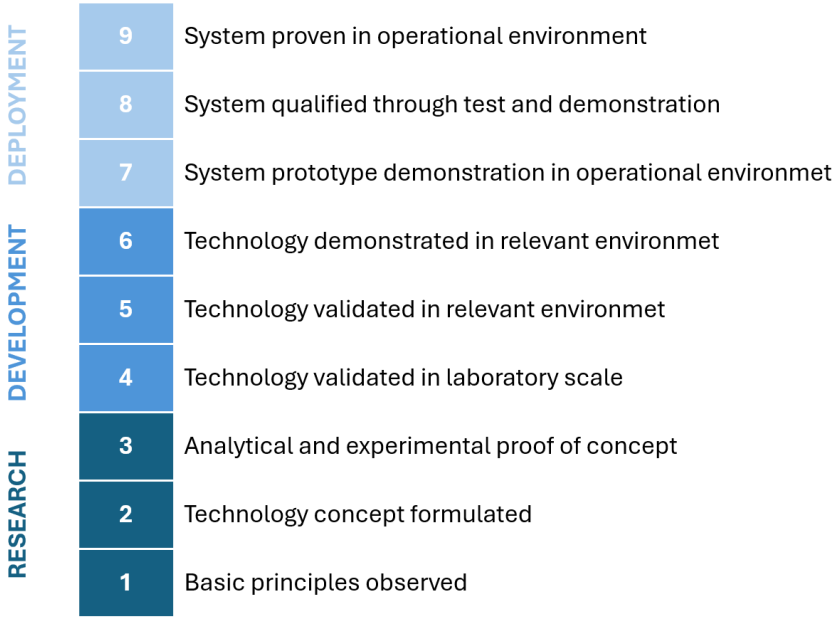

Figure 4. Technology Readiness Level (TRL) methodology for the validation of new technologies [19].

The use of the TRL methodology is widely spread in the research and development of new technologies and defines the basic requirements for each level of maturity in development. The purpose of this article is to present the results obtained at step 5, the current maturity level of the project, which supported the decisions to define the engineering of the demonstration plant (TRL 6) [19].

In addition to the analysis methodology mentioned for technology development, the New Wave Tech laboratory boasts various equipment and good process analysis practices. The experimental procedure and the equipment used in the analyses conducted in this article are discussed in the following sections.

2.1 Bauxite Residue (BR)

Approximately 15 tonnes of bauxite residue (BR) was collected from Hydro Alunorte in Barcarena, PA, Brazil, after the press filter process, then shipped to the Tech Center in Duque de Caxias, RJ, Brazil. To create a representative sample, 30 samples of 15 kg each were collected from different parts, combined into a single sample, and then homogenized and quartered using elongated and conical.

5 kg sample was quartered following the procedure shown in Figure 5. An aliquot of 500 grams was taken for chemical analysis. The remaining material was wet sieved using sieves of 150 microns, 75 microns, 45 microns, 32 microns, and 20 microns for granulometry analysis.

Figure 5. Representative sample received from Hydro Alunorte, homogenized, and quartered for characterization and tests.

2.2 Characterization of materials

The characterization techniques used in this paper are listed below:

X-ray diffraction (XRD): For Pig Iron the measurements were performed in a PANalytical AERIS instrument, with a cobalt-sealed ceramic X-ray tube (Kα1 = 1.78901 Å). For bauxite residue the measurements were performed in a PANalytical Empyrean with a θ-θ goniometer and a cobalt-sealed ceramic X-ray tube (Kα1 = 1.78901 Å). The instrumental conditions were as follows: voltage of 40 kV, scan runs of 5–80º (2θ), step size of 0.02º with a time/step of 20 s. For all samples, HighScore Plus software was used to identify the crystalline and quantification of present phases.

X-ray fluorescence spectrometry (XRF): Samples were prepared and analysed by X-ray fluorescence (XRF) using a Claisse electric fusion machine and a PANalytical Epsilon 1 instrument, ensuring precise analysis of total oxide contents. The loss on ignition (LOI) was determined by burning of the sample at 1000 °C.

Particle Size Analysis: The particle size distribution of samples was evaluated by a Bettersizer ST laser particle analyser, ensuring precise characterization of particle sizes.

Scanning Electron Microscopy with Energy-Dispersive X-ray Spectroscopy (SEM-EDS): For detailed analysis of morphological and mineral liberation characteristics, we utilize scanning electron microscopy with energy-dispersive X-ray spectroscopy (SEM-EDS) using a Hitachi TM4000Plus instrument, as well as optical microscopy for rapid and effective visual exploration.

Moisture: For determining the moisture content in minerals and process products, we used either the OHAUS MB-27 balance or a drying oven at 105 °C, ensuring precise and reliable results.

***Solid Digestion for Elemental Analysis*:** Samples undergo triacid digestion (HCl, HNO_3, HF) in an Anton Paar Multiwave 5000 microwave digester, providing efficient extraction of constituents for subsequent analyses.

Elemental Analyses by ICP-OES and AAS: Digested samples were analysed by atomic absorption spectroscopy (AAS) on an Agilent 200 Series AA instrument, or by inductively coupled plasma optical emission spectroscopy (ICP-OES) on an Agilent 5800 instrument, depending on the expected concentrations and required multi-element coverage.

Carbon and Sulfur Analysis: Total carbon content determination in samples was performed using an Eltra Elementrac CS instrument, allowing for precise characterization of constituents.

All reagents employed in this study were of analytical grade, ensuring the accuracy and reliability of the results. Solutions were meticulously prepared using ultrapure water from the Permution Aquapur Evolution system. To ensure the robustness of the analytical methods, specific Certified Reference Materials (CRMs) for iron ores, and bauxite were utilized.

3. Results and Discussion

Figure 6 shows the X-ray diffractogram of bauxite residue. It is observed that bauxite residue is mainly composed of Hematite (main peaks → $d_{10\text{-}2}$ = 3.68 Å, d_{104}= 2.7 Å, d_{110}= 2.52 Å) according to COD ID 96-901-5965; Sodalite (main peaks → d_{011} = 6.4 Å, d_{121}= 3.69 Å) according to COD ID 96-900-5051; Gibbsite (main peak → d_{002} = 4.84 Å) according to COD ID 96-101-1082; Goethite (main peak → d_{101} = 4.16 Å) according to COD ID 96-900-2160. The qualitative characterization results show that the BR is composed of the following mineral phases: Hematite (43%); Sodalite (20%); Al-Goethite (18%); Gibbsite (8.5%).

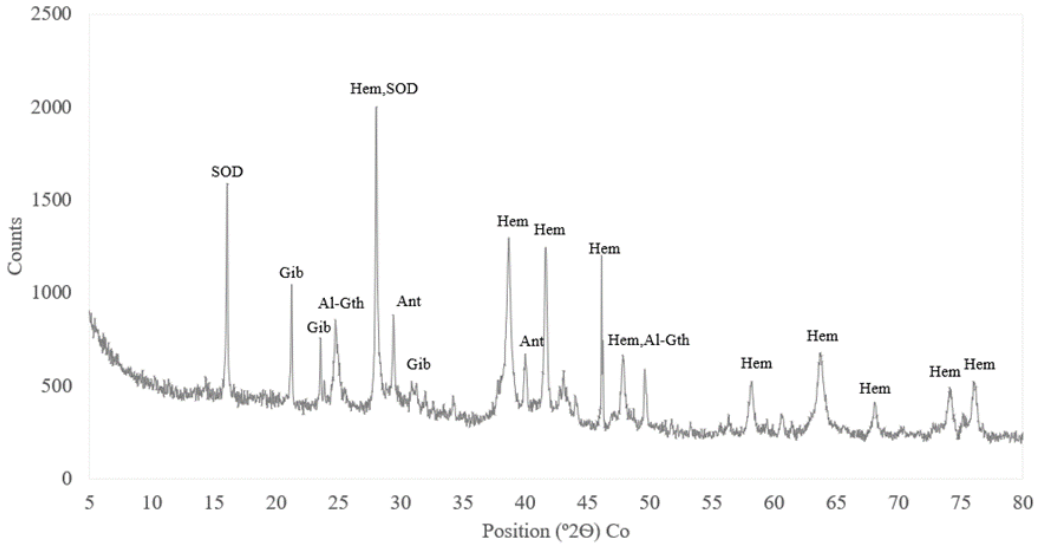

Figure 6. XRD of bauxite residue: Hem – hematite; SOD – sodalite; Gib – gibbsite; Al-Gth – Goethite Al; Ant – Anatase

The chemical composition of bauxite residue is shown in Table 2. SiO_2, Al_2O_3, Fe_2O_3, Na_2O and TiO_2 are main constituents. SiO_2, Al_2O_3 and Na_2O are related to sodalite structure. Al_2O_3 are related to gibbsite, also. Fe_2O_3 is related to hematite and goethite. TiO_2 is related to anatase structure. The chemical composition of bauxite residue corroborates the mineralogical characterization observed in the diffractogram of Figure 6.

Also, through Table 2, it can be confirmed that the bauxite residue is quite fine. In wet sieving, about 76.8 % of the total mass is below 20 µm.

Table 2. Chemical analysis of oxides by fraction of Hydro Alunorte bauxite residue using ED-XRF.

Fraction	Weight (%)	Na_2O (%)	Fe_2O_3 (%)	Al_2O_3 (%)	SiO_2 (%)	TiO_2 (%)	V_2O_5 (%)	ZrO_2 (%)	L.O.I.
+150 µm	3.75	3.54	45.24	10.75	28.76	3.14	0.18	0.17	6.55
-150 µm +75µm	3.78	4.47	45.78	8.78	13.34	16.95	0.27	2.56	4.97
-75 µm +45µm	4.29	3.31	44.61	11.15	11.03	12.62	0.24	5.96	5.75
-45 µm +38µm	1.31	7.10	40.38	14.46	10.84	10.11	0.22	5.15	7.66
-38 µm +20µm	10.08	4.03	31.98	30.55	10.57	6.26	0.15	2.07	13.86
-20µm	76.80	7.17	38.27	22.32	16.11	5.42	0.16	0.32	10.03
Total Sample	100.00	6.45	38.48	21.62	15.63	6.22	0.17	0.88	9.88

Using the particle sizer analyzer equipment, it was determined that the material is finer, Figure 5 shows that about 90 % of the particles are below 21.07 µm ± 0.30 µm. The laser diffraction analyzer provides more precise results as it is less affected by physical interferences compared to screen sieving, the overlapping of the cumulative size analyses is almost the same, and the particle size distribution is bimodal and fine in all replications. This result confirms the fine particle size of the material, suggesting that handling should be carefully selected to avoid overloading the dust collection system during material beneficiation.

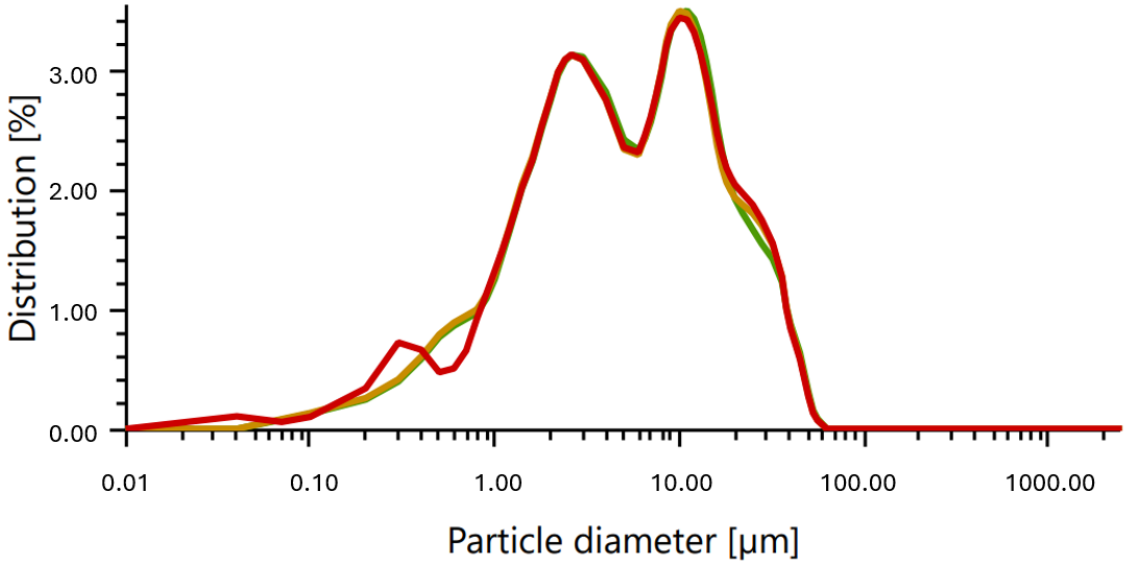

Figure 5. Frequency distribution in triplicate of the head sample using a particle analysis device by laser diffraction.

3.1 A Microwave Plant Assembly Process

The main unit operations that comprise the Wave Aluminium process is presented in Figure 6, along with the key parameters considered for the equipment sizing and engineering for the construction of a 50 000 tonne per year plant, providing a throughput of 6.25 tonnes of bauxite residue per hour, to be installed at Hydro-Alunorte. The main unit operations will be discussed in this section.

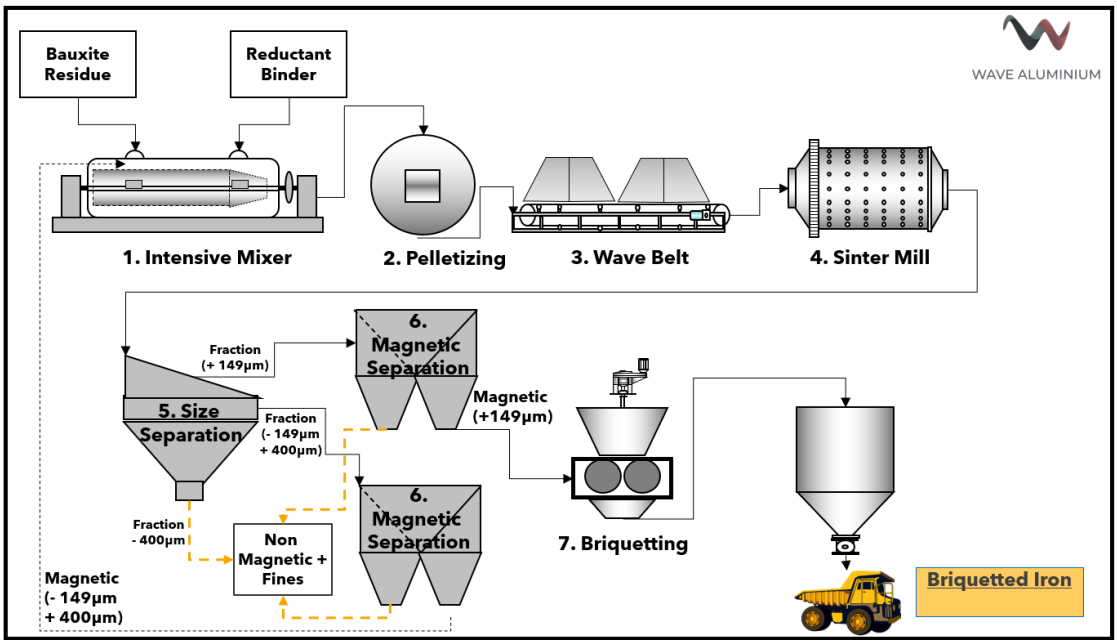

Figure 6: Process flow diagram for bauxite residue beneficiation developed by Wave Aluminium.

a. Intensive Mixer: The beneficiation process developed by Wave Aluminium, as shown in Figure 6, begins with an intensive mixing stage. This mixing was performed using two types of equipment to test their efficiency. The first equipment, the Ribbon Blender, demonstrated that the mixture was not completely homogeneous, with observable lump formation. In contrast, the intensive mixer, Figure 7, achieved a homogeneous, lump-free mixture with just one minute of residence time. This step is critical as a uniform mixture ensures the efficiency and consistency of subsequent processing stages.

a) b) c)

Figure 7. Stage of carbothermic mixture. a) Tested 70-liter mixer, b) Feeding of the carbothermic mixture, c) Mixture with adequate homogeneity after 1 minute of residence time.

The carbothermic reduction process, like any chemical process, depends on the contact between reagents meeting for the chemical reaction to occur. Thus, the degree of homogenization of the mixture directly influences the reduction process. In the mixture, bauxite residue with a moisture content of approximately 22 % to 23 % is added, along with 2.5 times the stoichiometric ratio of charcoal source relative to iron oxides. To reduce the slag viscosity, facilitating the iron agglomeration, dolomitic limestone is added, with the quantity defined by the bauxite residue composition. The strength of the raw pellets is increased by adding binders, which can be bentonite, sodium silicate, or hybrid binders, up to 1.0 % binder mass per mixture mass. Ensuring the proper proportion and thorough mixing of these additives is critical to optimize the reduction efficiency and improve the quality of the final product.

b. Pelletizing: In the pelletizing stage, with the addition of the elements from the carbothermic mixture, the moisture content drops to around 15 % and is adjusted on the disc to form pellets with an average size between 10 and 16 millimeters. This adjustment in moisture content is crucial to ensure the pellets achieve the desired mechanical strength and handling required for subsequent processing steps. Proper pellet formation enhances the efficiency of the reduction process by providing a uniform size distribution and optimal reactivity.

In the pelletizing stage, the carbothermic mixture produced by intensive mixing is fed by a silo. The disc inclination angle of 65° was determined to be the most effective for forming pellets within the defined range. With a moisture content of 19 to 21 %, the production rate of pellets is approximately 1 tonne of pellets per m² per hour. Using the equipment a) of the Figure 8 the flow rate met the specifications of the pellet production plant.

a) b) c)

Figure 8. Pelletizing process equipment. a) Pelletizing disc purchased for installation in the demonstration plant (3.9 meters in diameter), b) Pelletizing disc for determining pelletizing parameters (1.0 meters in diameter), c) Pellets formed under optimal conditions within the 10 to 16 mm range.

c. Wave Belt: The selection of equipment for the reduction process was the most complex part of the development process. Initially, a pilot rotary kiln was used for the reduction of pellets; however, the dispersion of microwaves and their propagation efficiency along the rotary kiln were low, making scaling up difficult. To overcome TRL 04 and 05, we deemed it necessary that the unit tested at TRL 05 be only continuous replicas to reduce the risk of scaling up. Therefore, a microwave cavity was optimized, and a conversion belt unit named “Wave Belt” was developed. This innovation ensures a more uniform and efficient microwave application, minimizing scalability risks and enhancing overall performance of the reduction process.

The first equipment tested for the reduction process was the cavity provided by the company that produces of the microwave sources. However, for the reduction process, it showed poor dispersion. Due to this, thousands of performances, dispersion, and operational condition tests were conducted to optimize microwave dispersion in the reaction bed. As the tests evolved, a specific cavity was defined, and TRL 05 tests were developed on a batch scale equipment with 100 kW power, resulting in the Wave Belt engineering construction equipment. The data generated from the Prototype 02 fed a dispersion model simulated in Ansys HFSS, which was used to improve the equipment. The continuous scale Wave Belt is in its final phase of completion and will be tested over the next two semesters to reduce the ramp-up time for the demonstration plant. Figure 9 shows the evolution of reduction cavities for the Wave Belt reduction equipment.

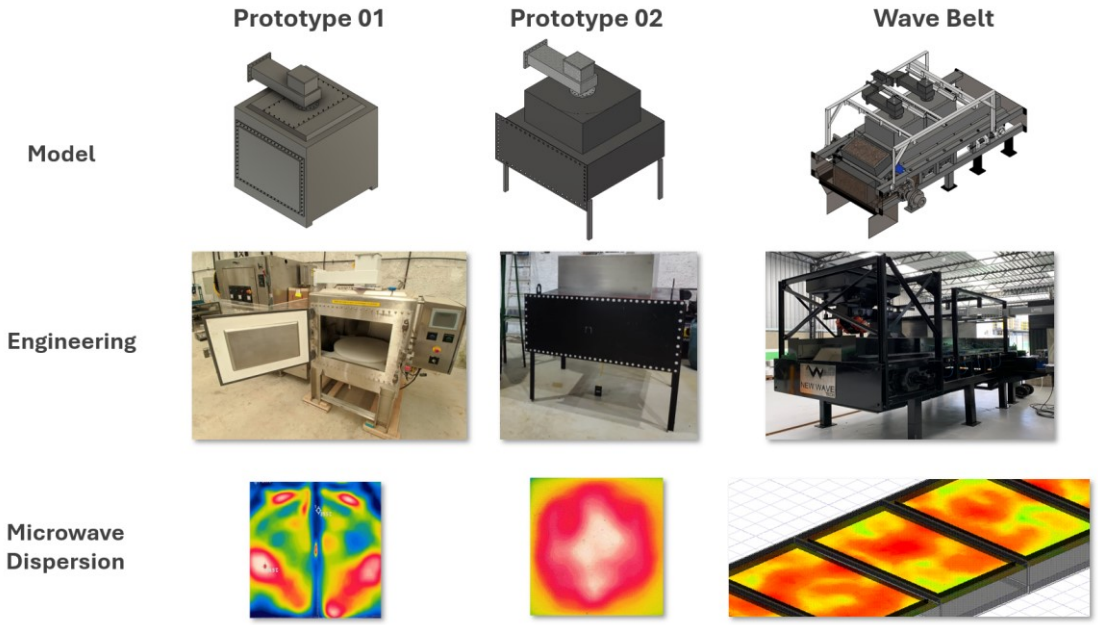

Figure 9. Evolution of reduction cavities for the Wave Belt reduction equipment. Prototype 01 and Prototype 02 the microwave dispersion is from thermal camera and Wave Belt the microwave dispersion was simulated in Ansys HFSS using the prototype 02 database.

Under the best reduction conditions, the result of processing 200 kg of the carbothermic mixture can be seen below, Figure 10.

a) b)

Figure 10: Large-Scale Reduction Tests. Left: a) Wave dispersion in the reaction bed after 15 minutes of microwaves (50 kg per batch and 40 kW), Right: b) Result of pilot-scale processing.

d. Comminution: After the pilot-scale carbothermic reduction process, the reduced material was crushed using a jaw crusher with a 5 mm opening, producing a carbothermically reduced material with the following granulometry and fraction composition, as shown in Table 3 below. This step ensures the material was prepared to the desired particle size distribution, optimizing it for further processing and analysis. The analysis that generated the data for the 1.18 mm fraction input, as an example, can be seen in Figure 11. This figure illustrates the detailed results of the granulometric and compositional analysis, providing insight into the distribution and quality of the reduced material at this specific particle size.

Table 3. Mineral liberation analysis (MLA) after carbothermal reduction and crushing, Figure 10-b.

Fraction (mm)	Weight (%)	Iron (%)	Ti-O (%)	Al-O (%)	Fe-O (%)	FeTi-O (%)	AlFe-O (%)	Silicates +Slag (%)
+1.18	26.9	56.82	0.1	0.43	3.97	0.19	0.27	36.39
-1.18+0.6	28.0	16.83	0.09	1.03	5.26	0.23	0.85	71.73
-0.6+0.3	17.1	16.51	0.06	0.74	5.38	0.28	0.91	73.21
-0.3+0.15	12.7	14.72	0.25	1.11	6.57	0.48	1.27	72.5
-0.15 +0.075	8.0	18.8	0.39	1.65	6.71	0.71	1.32	67.84
-0.075 +0.038	5.7	8.47	0.21	1.9	6.18	0.51	1.49	77.06
-0.038	1.6	NA	NA	NA	NA	NA	NA	NA
	100.0	26.68	0.14	0.91	5.19	0.31	0.82	61.46

Table 3 and Figure 11 show that the coarser fractions retain a higher amount of metallized iron. This occurs because, after the reduction process to metallic iron, the iron particles create plasmas among themselves, increasing the temperature and consequently agglomerating the iron. The use of dolomitic limestone reduces the slag viscosity, facilitating the encounter and subsequent agglomeration of these reduced particles. It was also observed that the percentage of incompletely reduced iron oxide (FeO) is low, and the formation of undesirable phases such as FeTi-O and AlFe-O is minimal in the reduced material. These findings highlight the effectiveness of the reduction process and the role of additives in enhancing the quality of the product.

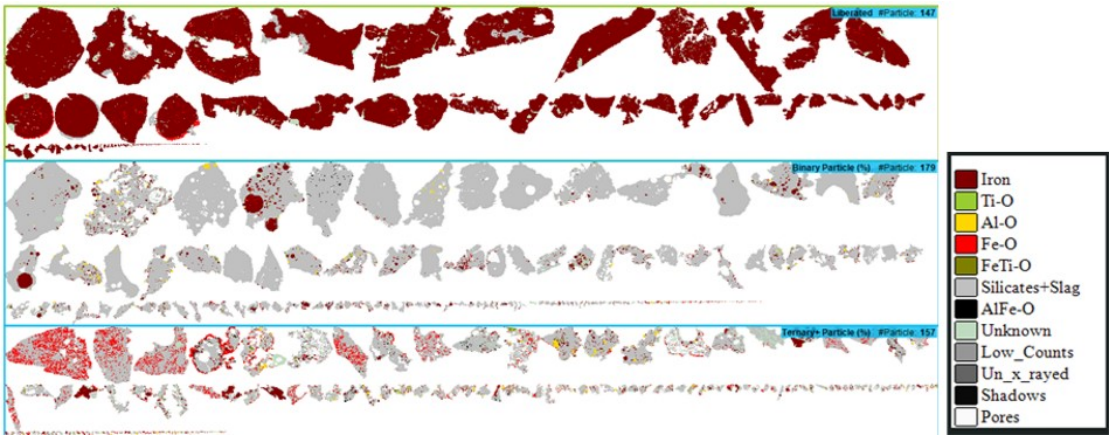

Figure 11. Iron liberation analysis (Gaudin-MLA) of the +1.18 mm fraction after carbothermic conversion, crushing, and screening.

e. Magnetic separation: After crushing the material and performing low-intensity magnetic separation, the product meets the specification with a high iron content and low impurity levels.

This final processing step ensures that the resulting product is of high quality, suitable for steelmaking applications. The analysis of the material, the product, which was sent for briquetting tests can be seen in Figure 12. This analysis provides detailed insights into the composition and quality of the material, ensuring it meets the necessary criteria for successful briquetting.

Figure 12. Left: a) Digital and b) optical microscope views. Coarse metallic iron agglomerates (150 µm size, with over 95% Fe Grade), Middle: c) and Right: d) SEM morphology analysis after reduction (150 µm).

Iron has different grinding characteristics compared to slag; iron tends to flatten while slag reduces in particle size. This difference makes low-intensity magnetic separation highly efficient. The magnetic properties of the 150 µm fractions can be seen in the XRD analysis (Figure 13). This analysis highlights the distinct separation achieved, emphasizing the effectiveness of the magnetic separation in isolating high-quality iron from the slag.

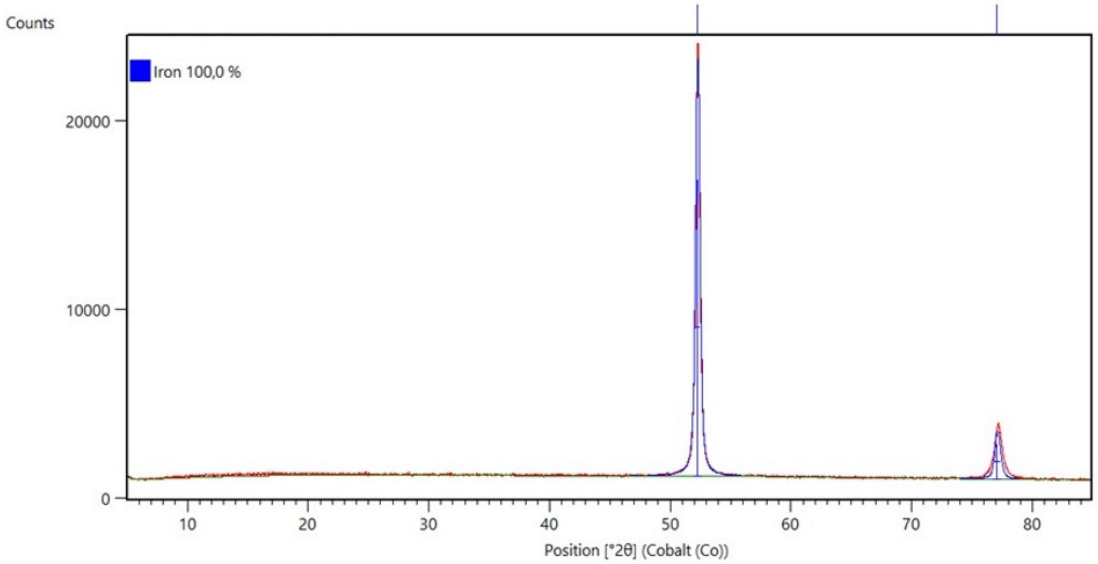

Figure 13. XRD analysis with a cobalt cathode and Rietveld refinement of the metallic magnetic fraction above 150 µm. Some minor phases may not be sufficient in volume to appear in the diffractogram.

f. Briquetting: The reduced material generated in the reduction tests was sent to the briquetting machine supplier unit for binder testing and to obtain parameters of the produced briquette.

The composition of the briquettes can be seen in Table 4, the column “Wave Aluminium Process” refers to the material reduced in the process before briquetting, and the column “Briquetted WA” refers to the properties of the briquettes, which are the product of the Wave Aluminium process.

The briquette with these specifications can feed both the basic oxygen furnace (BOF) or electric arc furnace (EAF) for steel production.

Table 4. Composition of the Briquettes Produced at the End of the Wave Aluminium Process

Elements	Wave Aluminium (WA) Process	Briquetted WA
Fe (%)	95.40	92.11
Metallization Degree (%)	+90.00	+90.00
P (%)	0.08	0.08
S (%)	0.08	0.08
C (%)	0.10 a 0.25	0.10 a 0.25
Non-magnetic (%)	< 0.80	-
$SiO_2 + Al_2O_3$ (%)	2.00 to 5.00	1.5 to 5.0
CaO + MgO (%)	0.05 to 0.80	+1
Size (mm)	0.10 to 4.00	-
Volume (cm^3)	-	10
Density (g/cm^3)	-	3.45 to 3.70
Application	-	BOF + EAF

The culmination of various stages in the beneficiation process of bauxite residue, starting from pilot tests conducted at New Wave Tech and validated by major equipment suppliers, has propelled the process beyond TRL 5. The successful validation of the prototype in a relevant environment has led to the engineering development for assembling a demonstration plant, Figure 14, at a designated area within Hydro Alunorte. This progression underscores the tangible strides made in advancing the utilization of bauxite residue, marking a significant milestone in sustainable waste management practices within the industry.

Figure 14: Layout of the Wave Aluminium 50 000 tons per year demonstration plant.

4. Conclusions

Wave Aluminium's process for demonstration plant assembly has been validated with operational parameters were demonstrated at scale-up for the main Unit Operations. Below are the main conclusions:

Utilizing microwave energy and charcoal has been technically feasible for reducing the iron oxides present in bauxite residue and subsequently separating the metallic iron, thereby generating a product with significant demand.

The use of electrical energy and charcoal results in lower emissions compared to conventional processes for producing iron. Life cycle analysis studies are underway to validate the extent of emission reduction, along with instrumentation at the outputs of the demonstration plant to monitor and control these gases.

The non-magnetic material rich in nepheline and fly ash (from combustion) represents a potential co-product that could find application in the construction industry, which also consumes large volumes.

The conducted tests have provided documentation to reach TRL 5 maturity level and establish parameters for the engineering of the demonstration plant.

5. References

1. Guo-tao Zhou et al., Toward sustainable green alumina production: a critical review on process discharge reduction from gibbsitic bauxite and large-scale applications of red mud, *Journal of Environmental Chemical Engineering*, Volume 11, No. 2, (2023), 109433.
2. Adela Svobodova-Sedlackova et al., Mapping the research landscape of bauxite by-products (red mud): An evolutionary perspective from 1995 to 2022, *Heliyon*, Volume 10, No. 3, (2024), e24943, https://doi.org/10.1016/j.heliyon.2024.e24943.
3. PT Cita Mineral Investindo Tbk, *Jakarta*, (2021) https://www.citamineral.com/investor/reports (Accessed on 01/08/2024).
4. Fathi Habashi, A hundred years of the Bayer process for alumina production. In: D. Donaldson and B. E. Raahauge (eds) *Essential readings in light metals*. Springer, Cham, 2016.
5. Huang Lingxiang et al., Research progress on comprehensive utilization of red mud, *Journal of Physics: Conference Series,* Vol. 2009, No. 1, (2021), 012021, https://doi.org/10.1088/1742-6596/2009/1/012021.
6. International Aluminium Institute, *Sustainable bauxite residue management guidance* (2022), https://international-aluminium.org/resource/sustainable-bauxite-mining-guidelines-second-edition-2022-2/ (Accessed on 01/08/2024)
7. Council of the EU, Press release 30 June 2023 https://www.consilium.europa.eu/en/press/press-releases/2023/06/30/critical-raw-material-act-council-adopts-negotiating-position/ (Accessed on 01/08/2024).
8. International Aluminium Institute, *Bauxite residue: an introduction factsheet*, https://international-aluminium.org/resource/bauxite-residue-an-introduction-factsheet/ (Accessed on 01/08/2024)
9. Ken Evans, The history, challenges, and new developments in the management and use of bauxite residue, *Journal of Sustainable Metallurgy,* Vol. 2, No. 4, (2016), 316–331.
10. Tomoko Radomirovic et al., Crystallization of sodalite particles under Bayer-type conditions, *Hydrometallurgy*, Vol. 137, (2013), 84–91.

11. V P Gridasov et al., Behavior of alkalis in blast furnaces, *Metallurgist,* Vol. 59, No. 9-10, (2016), 761–765.
12. Matic Jovičević-Klug et al., Green steel from red mud through climate-neutral hydrogen plasma reduction, *Nature,* Vol. 625, No. 7996, (2024), 703–709.
13. Angel Lopez, *Demonstration of BR microwave roasting in prototype furnace*, (2023), https://cordis.europa.eu/project/id/776469/results (Accessed on 01/08/2024).
14. Lena Mazeina and Alexandra Navrotsky, Surface enthalpy of goethite, *Clays and Clay Minerals,* Vol. 53, No. 2, (2005), 113–122.
15. Gabriel Plascencia and David Jaramillo, *Basic thermochemistry in materials processing,* 1st edition, Springer, Mexico City, 2016.
16. Wolfram Research, *ChemicalData, Wolfram Language function*, (2007), https://reference.wolfram.com/language/ref/ChemicalData.html (updated 2016) (Accessed on 01/08/2024).
17. Dawei Yu et al., TG/DTA study on the carbon monoxide and graphite thermal reduction of a high-grade iron nickel oxide residue with the presence of siliceous gangue, *Thermochimica Acta*, Vol. 575, (2014), 1–11.
18. Jacob Hunt et al., Microwave-specific enhancement of the carbon–carbon dioxide (Boudouard) reaction, *The Journal of Physical Chemistry C* 2013 Vol. 117, No. 51, (2013), 26871-26880.
19. John C. Mankins. *Technology readiness levels. A White Paper*, NASA, Washington, DC, 1995.